ISSN (Print) : 2320 – 3765
ISSN (Online): 2278 – 8875

International Journal of Advanced Research in Electrical, Electronics and Instrumentation Engineering
Vol. 2, Issue 7, July 2013

POWER FACTOR CORRECTION WITH BOOST RECTIFIER

Dr.K.Ravichandrudu[1] , P.Suman Pramod Kumar [2], M.Sailaja[3], M.Meena[4]

Professor, Dept. of EEE, Krishnaveni Engineering College, Guntur, India[1]

Associate Professor, Dept. of EEE, CR.Engineering College,Tirupati, India[2]

PG Student, Dept of EEE, CR.Engineering College, Tirupathi, India[3]

PG Student, Dept of EEE, CR.Engineering College, Tirupathi, India[4]

ABSTRACT : Conventional AC/DC power converters that are connected to the line through full-wave rectifier draws a non-sinusoidal input current. These Harmonic currents flowing through the impedances in the electrical utility distribution system can cause several problems such as voltage distortion, heating, noises. These harmonics distort the local voltage waveform, potentially interfering with other electrical equipment connected to the same electrical service and reduce the capability of the line to provide energy. This fact and the presence of standards or recommendations have forced to use power factor correction in power supplies. Boost regulators have been with us for many years as a power factor correction rectifiers. The main problem in boost rectifier is, the output voltage is very sensitive to Duty ratio variations. So maintaining the output voltage with in the regulation is very complex. Boost regulators are draws power from utility at unity power factor when it is operated in continuous conduction mode.

Key words: Rectifier,power factor conduction mode,Modulator

I. INTRODUCTION

In this Paper, the Predictive Switching Modulator(PSM) for current mode control of high power factor boost rectifier is proposed. In this strategy the duty ratio of the switch is controlled in such a way that the estimated inductor current will be proportional to the rectifier input voltage at the end of the switching period(T_s). The estimation of the inductor current is possible since the input voltage is practically constant over a switching period. This enables us to predict the current ripple of the subsequent off period during the on time of the switch itself. The input current waveform gets distorted in the Discontinuous Conduction Mode(DCM) operation of the NLC controlled boost rectifier. The advantage of the PSM is the extended range of Continuous Conduction Mode (CCM) of operation compared to the NLC. The PSM modulator has the structure of a standard current programmed controller with compensated ramp that is nonlinear. The steady-state stability condition and the low-frequency small-signal model of the PSM switched boost rectifier are derived by applying standard graphical and analytical methods of the current mode control.

II. BASIC OPERATION OF THE BOOST RECTIFIER

The boost is a popular non-isolated power stage topology, sometimes called a step-up power stage. Power supply designers choose the boost power stage because the required output voltage is always higher than the input voltage, is the same polarity, and is not isolated from the input. The input current for a boost power stage is continuous, or non-pulsating, because the input current is the same as the inductor current. The output current for a boost power stage is discontinuous, or pulsating, because the output diode conducts only during a portion of the switching cycle. The output capacitor supplies the entire load current for the rest of the switching cycle. The power circuit of dc-dc Boost rectifier is shown in fig.1.

ISSN (Print) : 2320 – 3765
ISSN (Online): 2278 – 8875

International Journal of Advanced Research in Electrical, Electronics and Instrumentation Engineering
Vol. 2, Issue 7, July 2013

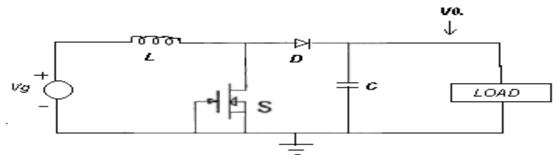

Fig. 1 Boost dc-dc Converter

When the switch is on, the diode is reversed biased, thus isolating the output stage. The input supplies energy to the inductor. When the switch is off, the output stage receives energy from the inductor as well as from the input.

The steady state analysis for continuous conduction and discontinuous conduction mode of operation is explained below.

A. Boost Power Stage Steady-State Analysis

A power stage can operate in continuous or discontinuous inductor current mode. In continuous inductor current mode, current flows continuously in the inductor during the entire switching cycle in steady-state operation. In discontinuous inductor current mode, inductor current is zero for a portion of the switching cycle. It starts at zero, reaches a peak value, and returns to zero during each switching cycle. The output filter capacitor is assumed to be very large to ensure a constant output voltage $v_0(t) \approx V_0$

B. Boost Steady-State CCM Analysis

The basic power circuit of boost converter during ON and OFF period is shown in Fig.2
Fig.3.shows the steady-state waveforms for this mode of conduction where the inductor current flows continuously [$i_l(t) > 0$].

Since in steady state the time integral of the inductor voltage over one time period must be zero,

$$V_0 t_{on} + (V_g - V_0) t_{off} = 0 \quad (1)$$

Dividing both sides by T_s and rearranging terms yields

$$\frac{V_0}{V_g} = \frac{T_s}{t_{off}} = \frac{1}{1-D} \quad (2)$$

Assuming a loss less circuit, $P_g = P_0$,

$$\therefore V_g I_g = V_0 I_0 \quad (3) \text{ and}$$

$$\frac{I_0}{I_g} = (1-D) \quad (4)$$

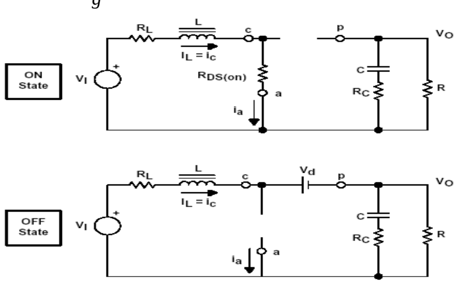

Fig.2.Boost power stage stages

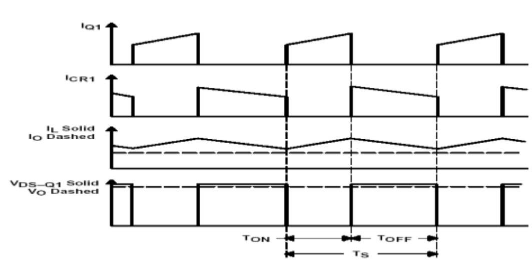

Fig.3. Continuous mode Boost power stage waveforms

ISSN (Print) : 2320 – 3765
ISSN (Online): 2278 – 8875

International Journal of Advanced Research in Electrical, Electronics and Instrumentation Engineering
Vol. 2, Issue 7, July 2013

C. Boundary Between Continuous and Discontinuous Conduction

Fig.4(a).Shows the waveforms at the edge of continuous conduction. By definition, in this mode i_l goes to zero at the end of the off interval. The average value of the inductor current at this boundary is

$$I_{lb} = \frac{1}{2} i_{l,peak} \quad (5)$$

$$= \frac{1}{2}\frac{V_g}{L} t_{on} \quad (6)$$

$$= \frac{T_s V_0}{2L} D(1-D) \quad \text{(using Eq 3.2)} \quad (7)$$

From Eq.3.4. and Eq.3.7 we find that the average output current at the edge of continuous conduction is

$$I_{OB} = \frac{T_s V_0}{2L} D(1-D)^2 \quad (8)$$

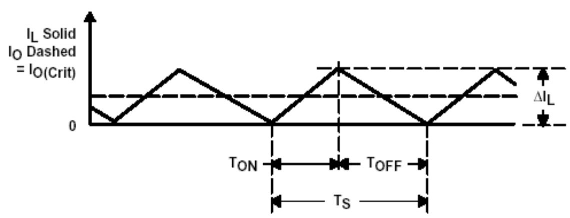

Fig. 4(a)Boost Converter at the boundary of Continuous-Discontinuous Conduction

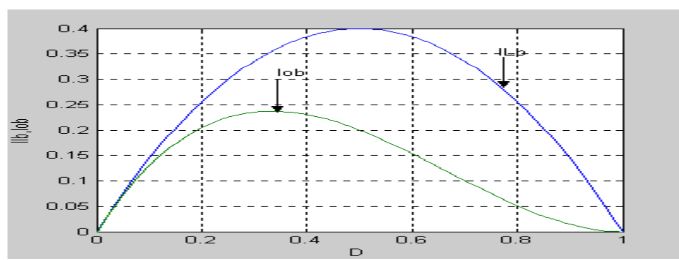

Fig.4(b). I_{oB} and I_{gB} with V_o constant by varying D

(9)

Also, I_{oB} has its maximum a*t $D=1/3=0.333$:*

$$I_{OB,\max} = 0.074 \frac{T_s V_0}{L} \quad (10)$$

In terms of their maximum values, I_{LB} *and* I_{OB} can be expressed as

$$I_{LB} = 4D(1-D) I_{LB,\max} \quad (11)$$

and

$$I_{OB} = \frac{27}{4} D(1-D)^2 I_{OB,\max} \quad (12)$$

Fig.4(b) shows that for a given D, with constant V_0, if the average load current drops below I_{OB} (and, hence, the average inductor current below I_{LB}), the current conduction becomes discontinuous.

D. Discontinuous conduction mode

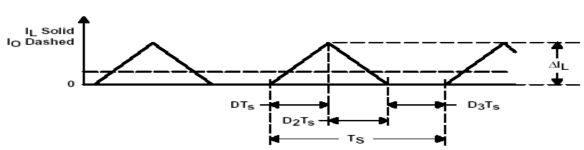

Fig. 5.Boost Converter Waveform at Discontinuous Conduction

ISSN (Print) : 2320 – 3765
ISSN (Online): 2278 – 8875

International Journal of Advanced Research in Electrical, Electronics and Instrumentation Engineering
Vol. 2, Issue 7, July 2013

In Fig.5 The discontinuous current conduction occurs due to decreased P_0 and ,hence, a lower I_L, since V_g is constant. Since $I_{L\ peak}$ is the same in both modes in Fig3.4 , and Fig.5. a lower value of I_L is possible only if V_0 goes up in fig.5.

If we equate the integral of the inductor voltage over one time period to zero,

$$V_g DT_s + (V_g - V_0)\Delta_1 T_s = 0$$

$$\therefore \frac{V_o}{V_g} = \frac{\Delta_1 + D}{\Delta_1} \qquad (13)$$

and

$$\frac{I_0}{I_g} = \frac{\Delta_1}{\Delta_1 + D} \qquad (14)$$

From Fig.3.5 ,the average input current, which is also equal to the inductor current, is

$$I_g = \frac{V_g}{2L} DT_s (D + \Delta_1) \qquad (15)$$

it is more useful to obtain the required duty ratio D as a function of load for various values of V_0/V_g . By using Eqs… , we determine that

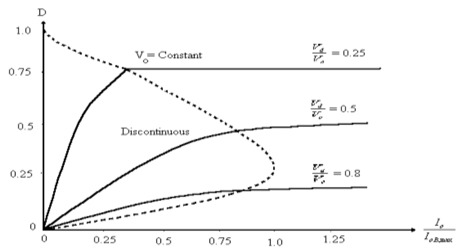

Fig. 6.Boost Converter characteristics keeping V_o constant

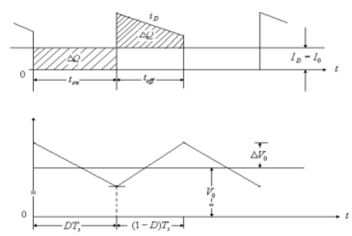

Fig. 7.Boost Converter out put voltage ripple

$$\frac{L}{2} i_{L,peak}^2 = \frac{(V_g DT_s)^2}{2L} \text{ W-s} \qquad (18)$$

are transferred from the input to the output capacitor and to the load. If the load is not able to absorb this energy, the capacitor voltage V_0 would increase until an energy balance is established.

E. Output Voltage Ripple

Therefore, the peak-peak voltage ripple is given by

$$\Delta V_0 = \frac{\Delta Q}{C} = \frac{I_0 DT_s}{C} \qquad (19)$$

$$= \frac{V_0}{R}\frac{DT_s}{C} \qquad (20)$$

ISSN (Print) : 2320 – 3765
ISSN (Online): 2278 – 8875

International Journal of Advanced Research in Electrical, Electronics and Instrumentation Engineering
Vol. 2, Issue 7, July 2013

F. Controlling Of Boost Rectifier

The various methods of power factor Correction can be classified as

(i) Passive Power Factor Correction techniques
(ii) Active Power Factor Correction techniques

1. Passive Power Factor Correction Techniue

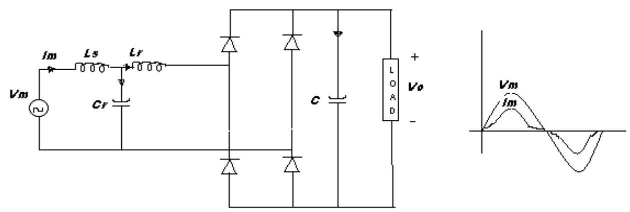

Fig. 8. The Passive Power factor correction technique

In this approach an L-C filter is inserted between the AC mains line and the input port of the diode rectifier of AC-to-DC converter as shown in Fig.8**.** This technique is simple and rugged but has bulky size and heavy weight and the Power Factor can not be very high.

2. Active Power Factor Correction Technique

The Power Factor can reach almost unity and the AC/DC interface of power converter emulates a pure resistor as shown in Fig.9. Comparing with the Passive Power Factor Correction methods, the Active Power Factor Correction techniques have many advantages such as, High Power Factor, reduced Harmonics, small size and light weight.

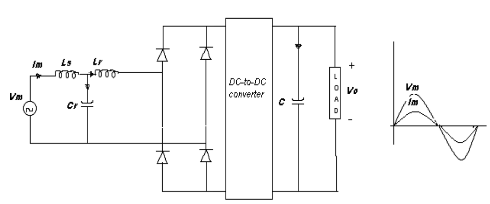

Fig. 9 The active power factor correction Technique

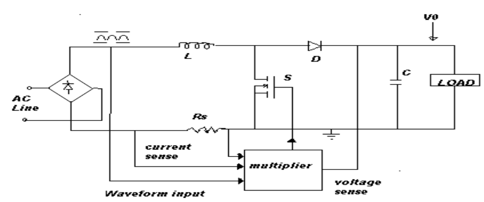

Fig. 10 Block diagram of PFC circuits at CCM operation with the Multiplier approach

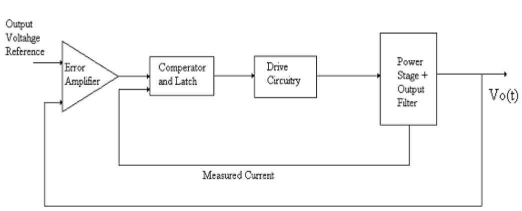

Fig. 11. Current Mode Control

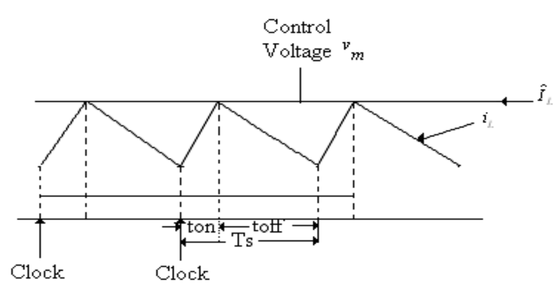

Fig. 12. Constant Frequency Control with turned-on at clock time

There are two basic controllers are proposed for the PWM power factor correction technique, namely, *Peak current mode control* and *Average current mode control* to boost converter operating in CCM .

ISSN (Print) : 2320 – 3765
ISSN (Online): 2278 – 8875

International Journal of Advanced Research in Electrical, Electronics and Instrumentation Engineering
Vol. 2, Issue 7, July 2013

3. Peak Current Mode Control:

This technique was proposed for boost converter operating at CCM mode with constant switching frequency as shown in fig. 13. It has all he advantages of the boost type configuration working at CCM mode. Te problem of this technique is its requirement of a slope compensation to stabilize the control system.

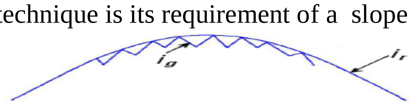

Fig 13. Peak Current Mode Control

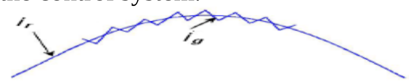

Fig 14. Average Current Mode Control

4. Average Current Mode Control

This technique was proposed for boost converter operating at CCM mode with constant switching frequency, as shown in fig. 14. It has all the advantages of the boost type configuration working at CCM mode. The demerit of this technique is current control system is complex and difficult to analyze and synthesize. In a simplified circuit was proposed to shape the sinusoidally varying average current without sensing the input voltage.

However, The *peak current mode controller* and *average current mode controllers* are suffering from the stability problem due to the presence of inherent sub harmonic oscillations if the duty ratio of the power switch is greater than 50% and noise immunity.

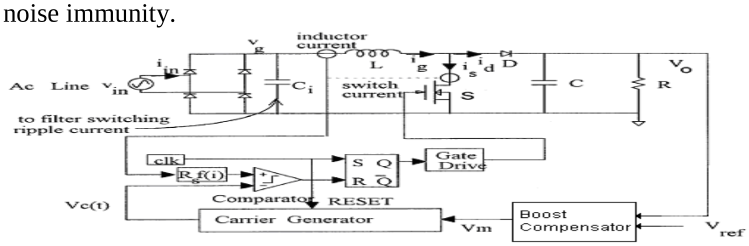

Fig. 15. Power circuit of the single phase PFC rectifier with the generalized control structure of the NLC, the LPCM, and the PSM.

5. Quasi Steady-State Approach

The line frequency in Fig.3.6**.** is usually well below the switching frequency, hence, the input voltage of the dc-dc converters can be approximated as a constant in a consecutive switching periods.. The important property of the quasi steady state operation is that all quantities can be approximated with their steady-state values.

The control objective of the resistor emulator is to force the input current of the dc-dc converter to be proportional to the input voltage so that the input impedance is resistive. In other words, the local average of the input current

$$\langle i_g \rangle = v_g / R_e \qquad (22)$$

where R_e is the emulated resistance. $<i_g>$ can be controlled by modulating the duty ratio d.

The objective given in (3.22) can be accomplished, in general, with the control law

$$R_s \langle i_g \rangle = v_m / M(d) \qquad (23)$$

due to the quasi-steady-state operation, where R_s is the equivalent current sensing resistance, *M(d)* is the voltage conversion ratio of the dc-dc converter, and v_m is the modulation voltage, as shown in Fig.3.15. for controlling the amplitude of the line current. When the CCM dc-dc converter is stable , the steady state duty ratio D satisfies

$$V_o / V_g = M(D) \qquad (24)$$

where V_o is the output voltage and *M(D)* for boost rectifier is $1/(1-d)$. Capital characters are used here to indicate the switching frequency steady state. Substituting (3.24) into (3.23) yields the quasi-steady-state approximation

$$R_s \langle i_g \rangle = v_m v_g / V_o \qquad (25)$$

ISSN (Print) : 2320 – 3765
ISSN (Online): 2278 – 8875

International Journal of Advanced Research in Electrical, Electronics and Instrumentation Engineering
Vol. 2, Issue 7, July 2013

V_o is a constant over a line cycle if the output capacitance is large enough; therefore, if v_m is also a constant in line cycle, $<i_g>$ is proportional to v_g and the emulated resistance

$$R_e = R_s V_o / v_m$$

Voltage v_m regulate R_e so as to control the input current.

III. PREDICTIVE SWITCHING MODULATOR(PSM)

The generalized control objective of a high power factor boost rectifier can be expressed as

$$f(i_g) = \frac{v_g}{R_e} \tag{26}$$

*R*e is the emulated resistance of the rectifier and is a function of the inductor current . This function can be different for different control strategies. For example NLC implements average current mode control, so for NLC (3.27) is the specific expression of $f(i_g)$

$$f(i_g)_{nlc} = i_{g,av(Ts)} = \frac{1}{Ts}\int_0^{Ts} i_g\, dt \tag{27}$$

$$f(i_g)_{lpcm} = i_{gp} = i_g\left[dT_s\right] \tag{28}$$

In the proposed modulator the duty ratio of the switch is controlled in such a way that the inductor current becomes proportional to the rectified input voltage at the end of each switching period. Therefore for PSM the function is given by

$$f(i_g)_{psm} = i_g\left[T_s\right] \tag{29}$$

Fig. 3.16 shows the generalized control objective of the boost rectifier.

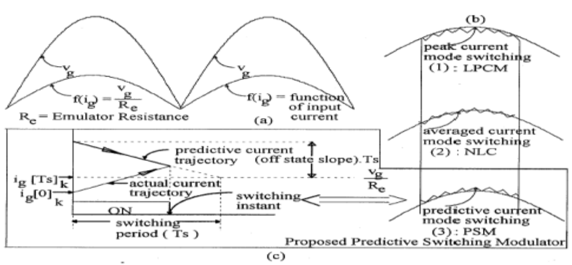

Fig. 16 Generalized control objective of the carrier-based current mode controllers

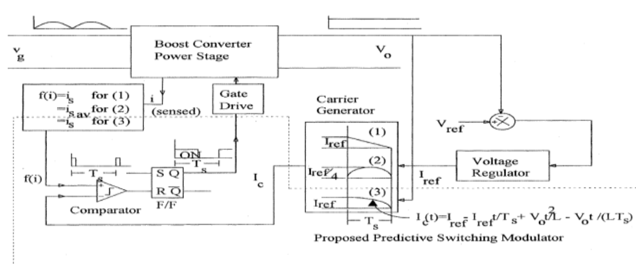

Fig. 17 Block Diagram of the carrier based input-current-shaping controllers: (the LPCK; 2) the NLC 3) the PSM

Operating principle of the PSM.

For a boost rectifier the switch current is equal to the inductor current during ON time of the switch. In a switching period $T_{s,}$ instead of the inductor current, it is convenient to average the switch current by carrying out integration only over the ON time of the switch because the switch current is zero during the rest of the period. Therefore the modulator of NLC implements the control law given by (28). For LPCM and PSM either the switch current or the inductor current can be sensed. The control laws for LPCM and PSM in terms of the switch current are given by

$$di_{g,av}(T_s) = \frac{1}{T_s}\int_0^{dT_s} i_g\, dt = \frac{1}{T_s}\int_0^{dT_s} i_s\, dt = d\,\frac{v_g}{R_e} \tag{30}$$

$$i_g(dT_s) = i_s(dT_s) = \frac{v_g}{R_e} \tag{31}$$

ISSN (Print) : 2320 – 3765
ISSN (Online): 2278 – 8875

International Journal of Advanced Research in Electrical, Electronics and Instrumentation Engineering
Vol. 2, Issue 7, July 2013

$$i_g[T_s]_k = i_s[0]_{k+1} = \frac{v_g}{R_e} \qquad (32)$$

It may be noted that the inductor current at the end of period is equal to the current at the beginning of the next period, or, $i_g[T_s]_k = i_g[0]_{k+1} = \frac{v_g}{R_e}$. Since that switching frequency of the converter is much higher than the frequency of the input voltage when the converter is operating in CCM the slope of the turn-off current can be predicted during ON time of the switch itself. Then instead of (32), (33) can be used for PSM

$$i_g[dT_s]_k = i_s[dT_s]_k = \frac{v_g}{R_e} + \left(\frac{V_o - v_g}{L}\right)(1-d)T_s \qquad (33)$$

We can use the boost converter continuous conduction mode input to output conversion equation of (3.34) to replace v_g in (3.33) by v_o and d . Then we get (3.35) as the duty ratio control function for the PSM

$$v_g = (1-d)V_0 \qquad (34)$$

$$i_g[dT_s] = I_{ref}(1-d) + \left(\frac{V_0 T_s}{L}\right)d(1-d) \qquad (35)$$

where

$$I_{ref} = \frac{V_0}{R_e} = \frac{v_m}{R_s} \qquad (36)$$

R_s is the current sense resistance of the converter and v_m is the input voltage to the modulator. Under closed loop operation is obtained as the output of the voltage error amplifier loop. In nlc and lpcm, the right-hand-side expressions of (3.27) and (3.28) are converted into suitable carrier waveforms by replacing the duty ratio term d by t/T_s .

Similarly the carrier waveform $I_c(t)$ for the predictive switching modulator can be expressed as

$$I_c = \frac{V_c(t)}{R_s} = I_{ref}\left(1-\frac{t}{T_s}\right) + \left(\frac{V_0 T_s}{L}\right)\frac{t}{Ts}\left(1-\frac{t}{T_s}\right) \qquad (37)$$

For $0 \le t \le T_s$

Steady state stability condition

A. Continuous conduction mode (CCM)

steady-state stability analysis presented in this section is Graphical in nature. have For deriving the steady-state stability condition for the current mode controlled dc–dc converter, the objective is to quantify the steady-state stability condition of the PSM switched boost rectifier in terms of circuit parameters and switching frequency of the converter.

The steady-state carrier waveform, shown in Fig. 18(a), is configured as a function of d=t/T_s, in the standard structure of

$$I_c(d) = I_{ref} + I_{comp(d)} \qquad (38)$$

$$= I_{ref} - M_x T_s d - M_y T_s d^2 \quad \text{for } 0 \le d \le 1 \qquad (39)$$

where

$$I_{comp}(d) = -I_{ref}d + \left(\frac{V_0 T_s}{L}\right)d(1-d)$$

$$= -M_x T_s d - M_y T_s d^2 \quad \text{for } 0 \le d \le 1 \qquad (40)$$ and

ISSN (Print) : 2320 – 3765
ISSN (Online): 2278 – 8875

International Journal of Advanced Research in Electrical, Electronics and Instrumentation Engineering
Vol. 2, Issue 7, July 2013

$$M_x = \frac{I_{ref}}{T_s} - \frac{V_0}{L} \tag{41}$$

$$M_y = \frac{V_0}{L} \tag{42}$$

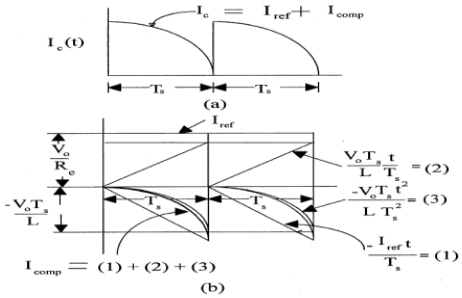

Fig.18 (a) Carrier Waveform of the PSM, (b) Current reference Iref and different components of the Compensating Waveform

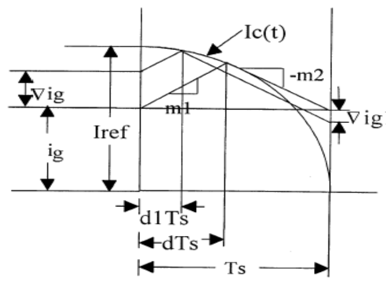

Fig19.Analysis of the steady state stability condition of the PSM switched boost rectifier

The following equations define the switching characteristics of the converter under steady and perturbed state:

$$i_g + m_1 d T_s = I_{ref} - M_x T_s d - M_y T_s d^2 \tag{43}$$

$$i_g + \nabla i_g + m_1 d_1 T_s = I_{ref} - M_x T_s d_1 - M_y T_s d_1^{\,2} \tag{44}$$

$$i_g + m_2(1-d)T_s = I_{ref} - M_x T_s d - M_y T_s d^2 \tag{45}$$

$$i_g + \nabla i_{g1} + m_2(1-d_1)T_s = I_{ref} - M_x T_s d_1 - M_y T_s d_1^{\,2} \tag{46}$$

$m_1>0$ and $m_2>0$ are magnitudes of the slopes in the inductor current during turn-on and turn-off intervals of the switch respectively. During the perturbation and are assumed to remain constant because the output voltage is constant and the input voltage is a slow varying quantity. For the boost converter m_1 and m_2 can be expressed as $m_1 = \frac{v_g}{L} = \frac{(1-d)V_0}{L}$ &

$$m_2 = \frac{V_0 - v_g}{L} = \frac{dV_o}{L}$$

from (3.2.5)-(3.2.8) we can get

$$\frac{\nabla i_{g1}}{\nabla i_g} = -\frac{m_2 - M_x - M_y(d+d_1)}{m_1 + M_x + M_y(d+d_1)} \tag{49}$$

In (49), we can replace m_1 , m_2,M_x,M_y, and I_{ref} by the expressions of (49), (41), (42), (47), and (48), respectively, in order to obtain

$$\frac{\nabla i_{g1}}{\nabla i_g} = 1 - \frac{1}{d_1 + \frac{L}{R_e T_s}} \tag{50}$$

Sub-harmonic oscillations in the boost rectifier can be avoided under the following condition:

$$\left|\frac{\nabla i_{g1}}{\nabla i_g}\right| < 1 \tag{51}$$

ISSN (Print) : 2320 – 3765
ISSN (Online): 2278 – 8875

International Journal of Advanced Research in Electrical, Electronics and Instrumentation Engineering
Vol. 2, Issue 7, July 2013

From (3.50) and (3.51), the steady-state stability condition for the PSM switched boost rectifier in terms of circuit parameters can be expressed as

$$\frac{2L}{R_e T_s} > (1-2d_1) \tag{52}$$

We assume that the perturbation is small, therefore $d_1 \approx d$. In CCM the duty ratio of the switch can be expressed as

$$D=(1-m_g), \text{ where } m_g = \frac{v_g}{V_0} \tag{53}$$

By combining (3.52) and (3.53), the steady-state stability condition can be obtained as

$$\frac{2L}{R_e T_s} > (2m_g - 1) \tag{54}$$

We need to replace R_e in (52) by the load resistance and other circuit parameters. For that the power balance condition $P_0=P_{in}$ between the input and output of the rectifier is used

$$p_{in} = \frac{2}{T}\int_0^{T/2} v_g i_{g,av(T_s)} T_s$$

$$= \frac{2}{T}\int_0^{T/2} v_g\left[\frac{v_g}{R_e} + \left(1-\frac{v_g}{V_0}\right)\frac{v_g T_s}{2L}\right]dt$$

$$= \frac{V_{gm}^2}{2R_e} + \frac{V_{gm}^2 T_s}{4L} - \frac{V_{gm}^3 T_s 4}{2LV_0 3\pi} \tag{55}$$

$$p_{out} = \frac{V_0}{R} \tag{56}$$

Here, T is the period of the line voltage waveform. Therefore by equating the expressions of (55) and (56) we get

$$\frac{R}{R_e} = \frac{2}{M_g^2} - \frac{T_s R}{2L}\left(1-\frac{M_g 8}{3\pi}\right) \tag{57}$$

where M_g is defined as

$$M_g = \frac{v_{g,Max}}{V_0} = \frac{V_{gm}}{V_0} \tag{58}$$

V_{gm} is the peak value of the rectified input voltage. We can also define K as

$$K = \frac{2L}{RT_s} \tag{59}$$

By combining (54) and (57), the steady-state stability condition of the PSM switched boost rectifier can be expressed as

$$K > M_g^2 (m_g - M_g \frac{4}{3\pi}) \tag{60}$$

It can be seen from (61), that the right-hand side expression is maximum when m_g or the rectified input voltage in a line cycle is maximum. The condition for avoiding sub-harmonic oscillations in the PSM switched boost rectifier over the entire cycle of the input voltage waveform is given by

$$K > K_{sp} = M_g^3\left(1-\frac{4}{3\pi}\right) \tag{61}$$

B. Discontinuous conduction mode (DCM)

ISSN (Print) : 2320 – 3765
ISSN (Online): 2278 – 8875

International Journal of Advanced Research in Electrical, Electronics and Instrumentation Engineering
Vol. 2, Issue 7, July 2013

In the DCM, the inductor current is zero at the beginning In the DCM, the inductor current is zero at the beginning of a switching period. Therefore the duty ratio of the period is determined by the modulator equation

$$\frac{v_g d T_s}{L} = I_{ref}(1-d) + \left(\frac{V_0 T_s}{L}\right) d(1-d) \qquad (62)$$

But in DCM,(3.34) is no longer valid. Instead

$$v_g < (1-d)V_0 \qquad (63)$$

Combining(65) and (66)we get (67) as the condition for the DCM

$$I_{ref} < 0 \qquad (64)$$

The expression of the average power($\tilde{P}$) due to the ripple current in the inductor (for $I_{ref}=0$) can be obtained from (55). It is given by

$$\tilde{P} = \frac{V_{gm}^2 T_s}{4L} - \frac{V_{gm}^2 M_g T_s 4}{2LV_0 3\pi} \qquad (65)$$

When the PSM switched boost rectifier is in the DCM, $I_{ref}<0$, and the output power $\left(V_o^2 / R < \tilde{P}\right)$. The condition for the DCM can be obtained as

$$K < K_{cp} = \left(\frac{M_g^2}{2} - M_g^3 \frac{4}{3\pi}\right) \qquad (66)$$

It can be concluded from (3.69), that $K \geq \left(\frac{M_g^2}{2} - M_g^3 \frac{4}{3\pi}\right)$ if the PSM switched boost rectifier remains in CCM over the entire duration, i.e.T/2 of the line half cycle. However, if the load resistance is such that $K < \left(\frac{M_g^2}{2} - M_g^3 \frac{4}{3\pi}\right)$ then the boost rectifier will operate stably in the DCM. In this mode a low-frequency pattern will appear in the steady-state waveform of I_{ref}.

In comparison, the NLC [3] controlled boost rectifier should satisfy (70) to support CCM over the entire half cycle of the input voltage waveform

$$K > K_{cn} = \frac{M_g^2}{2} \qquad (67)$$

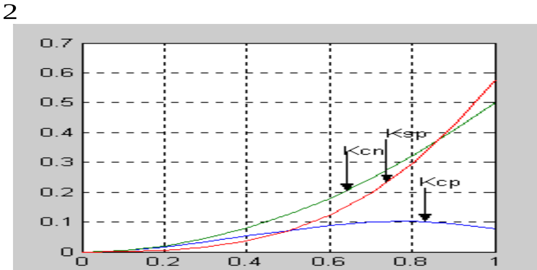

Fig. 20. Comparison of different critical k parameters: 1) K_{sp} steady state stability condition with the PSM; 2) K_{cp}: CCM operation with the PSM; and 3) K_{cn} CCm operation with the NLC.

K_{cp}, K_{cn} *and* ,K_{sp} and as functions of M_g are plotted in Fig. 3.20**.** K_{sp}values are valid only in the range in which CCM operation occurs, because such a condition has been used in its derivation.

ISSN (Print) : 2320 – 3765
ISSN (Online): 2278 – 8875

International Journal of Advanced Research in Electrical, Electronics and Instrumentation Engineering
Vol. 2, Issue 7, July 2013

IV. LOW FREQUENCY SMALL SIGNAL MODEL FOR PSM

In this section, we would like to develop a linear, low-frequency, small-signal model of the boost rectifier switched by the PSM In a line cycle, the rectified input voltage varies from 0 to v_{gm}. Under steady-state condition the inductor current I_g is proportional to rectified input voltage and the volt-second balance for the boost inductor occurs at every switching period (T_s).

The state space averaged model of the boost converter power stage is given by (26). We have used that model at the dc operating point of input voltage rms

$$\begin{bmatrix} \frac{dI_g}{dt} \\ \frac{dV_0}{dt} \end{bmatrix} = \begin{bmatrix} 0 & \frac{-(1-D)}{L} \\ \frac{(1-D)}{C} & \frac{-1}{RC} \end{bmatrix} \begin{bmatrix} I_g \\ V_0 \end{bmatrix} + \begin{bmatrix} \frac{1}{L} \\ 0 \end{bmatrix} [V_g] \tag{68}$$

where $V_g = \frac{V_{gm}}{\sqrt{2}}$

The steady state values of V_0 and I_g can be obtained from

$$V_0 = \frac{1}{(1-D)} V_g \tag{69}$$

$$I_g = \frac{1}{(1-D)^2 R} V_g \tag{70}$$

Our objective is to derive the control transfer function $G_v(s) = \hat{V}_o(s) / \hat{V}_m(s)$, the rectified input voltage V_g is not perturbed. Fig. 21 shows the schematic diagram of the method that has been used for deriving the control transfer function of the PSM switched boost rectifier

$$\begin{bmatrix} \frac{d\hat{I}_g}{dt} \\ \frac{d\hat{V}_0}{dt} \end{bmatrix} = \begin{bmatrix} 0 & \frac{-(1-D)}{L} \\ \frac{(1-D)}{C} & \frac{-1}{RC} \end{bmatrix} \begin{bmatrix} \hat{I}_g \\ \hat{V}_0 \end{bmatrix} + \begin{bmatrix} \frac{V_0}{L} \\ \frac{-I_g}{C} \end{bmatrix} [\hat{D}] \tag{71}$$

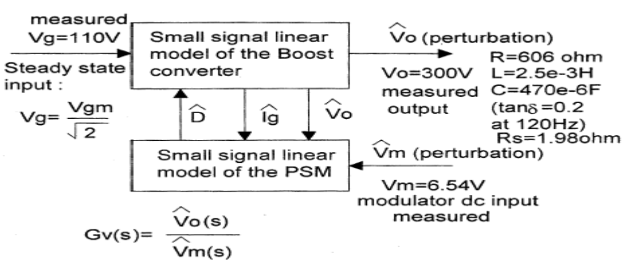

Fig. 21. Schematic diagram for derivation of the small signal linear model of PSM Switched boost rectifier for evaluation of the control gain transfer function $G_v(s)$

The modulator uses the inductor current I_g and the output voltage V_0 for producing the duty ratio of the period according to

$$V_m(1-D) + \frac{V_o R_s T_s}{L} D - \frac{V_o R_s T_s}{L} D^2 = I_g R_s + \frac{V_g R_s T_s}{2L} D \tag{72}$$

R_s is the sense resistance of the inductor current. The steady state duty ratio can be obtained (is the positive real root and less than 1) by solving

$$\left[-V_m + \frac{V_g R_s T_s}{2L}\right] D^3 + \left[3V_m - \frac{V_g R_s T_s}{L}\right] D^2 + \left[-3V_m + \frac{V_g R_s T_s}{2L}\right] D + \left[V_m - \frac{V_g R_s}{R}\right] = 0 \tag{73}$$

ISSN (Print) : 2320 – 3765
ISSN (Online): 2278 – 8875

International Journal of Advanced Research in Electrical, Electronics and Instrumentation Engineering
Vol. 2, Issue 7, July 2013

We perturb (3.76) and subsequently linearized the quantities to obtain the small-signal linear model of the PSM, as given by

$$\left[V_m + \frac{V_g R_s T_s}{2L} + 2DV_0\left(\frac{R_s T_s}{L}\right) - V_0\left(\frac{R_s T_s}{L}\right)\right]\hat{D} =$$

$$(1-D)\hat{V}_m + D(1-D)\hat{V}_0\left(\frac{R_s T_s}{L}\right) - \hat{I}_g R_s \qquad (78)$$

We define a constant N as fallows:

$$N = \left[\frac{V_m}{V_{m0}} + \frac{V_g R_s T_s}{2LV_o} + 2D\left(\frac{R_s T_s}{L}\right) - \left(\frac{R_s T_s}{L}\right)\right] \qquad (74)$$

We can rewrite (75) as (78) after replacing by the expression of (77) and using the definition of N

$$\begin{bmatrix} \frac{d\hat{I}_g}{dt} \\ \frac{d\hat{V}_0}{dt} \end{bmatrix} = \begin{bmatrix} \frac{-R_s}{LN} & \frac{-(1-D)}{L} + \frac{D(1-D)R_s T_s}{NL} \\ \frac{(1-D)}{C} + \frac{I_g R_s}{CV_0 N} & \frac{-1}{RC} - \frac{I_g D(1-D)R_s T_s}{CV_0 NL} \end{bmatrix} \begin{bmatrix} \hat{I}_g \\ \hat{V}_0 \end{bmatrix} + \begin{bmatrix} \frac{(1-D)}{LN} \\ \frac{-I_g(1-D)}{CV_0 N} \end{bmatrix} [\hat{V}_m]$$

(75)

The control gain transfer function can be obtained as shown in (3.81).

$$G_v(s) = \frac{-\left[\frac{s}{NRC} - \frac{(1-D)^2}{NCL}\right]}{s^2 + s\left[\frac{1}{RC} + \frac{DR_s T_s}{NRCL} + \frac{R_s}{NL}\right] + \left[\left(\frac{(1-D)^2}{LC}\right)\left\{1 - \frac{DR_s T_s}{NL}\right\} + \left\{\frac{2R_s}{NRLC}\right\}\right]}$$

(76)

The analytical model developed in this section is valid at any input–output and load condition as long as the boost converter operates in the continuous conduction mode.

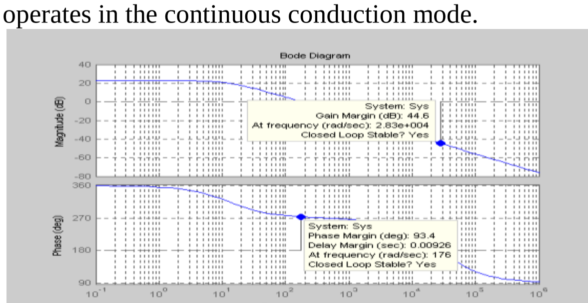

Fig. 22. Bode plot of the control gain transfer function $G_v(s)$ of the PSM switched boost rectifier

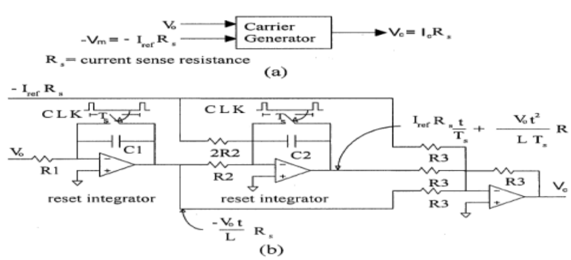

Fig. 23.(a) Carrier generator block of the PSM., (b) Circuit realization

Fig. 22shows the Bode plot of the control gain transfer function that is obtained by analysis. The dc input voltage of the modulator is V_m=6.54v. It produces an output voltage of V_0=300v, at V_g =110v and at load resistance of R=606Ω.

The control gain transfer function of nlc is first order that can effectively be used to design the frequency response of the voltage error amplifier. Usually for power factor correction circuit the closed loop bandwidth is chosen around 5–10 Hz. Therefore the small-signal model developed here, even though accurate for higher frequency of operation compared to that of dc-dc boost converter, has no added advantage so far as the design of the closed loop controller is concerned.

V.CONCLUSION

Boost regulator with predictive switching modulator works for high power ratings and extended range of continuous conduction mode operation.

ISSN (Print) : 2320 – 3765
ISSN (Online): 2278 – 8875

International Journal of Advanced Research in Electrical, Electronics and Instrumentation Engineering
Vol. 2, Issue 7, July 2013

VI.SIMULATION RESULTS

The Simulation work is done by using MATLAB/Simulink. The simulation diagram for the PFC Boost rectifier with PSM is shown in Fig.4.1. simulation result of the input current waveform is shown with the component values given by Table I. Form the Fig.4.2 by using the PSM we can get the THD in input current waveform is 6.08%

Table I

V_g	220V
V_0	300
L	25e-3
F_s	5000Hz
K	0.208
C	360e-5
R	1200

Fig.4.1 Simulation Block Diagram

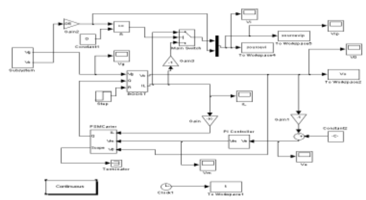

For 650 Ohm

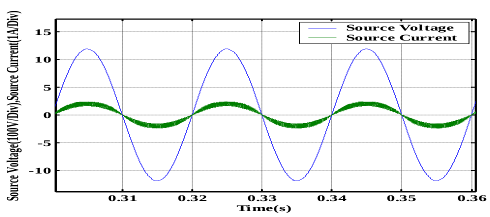

Fig. 4.2 Source current and voltage waveforms of the Boost Rectifier switc hed by the PSM at R=650Ω

For 650 ohms of resistance , source voltage and source currents are as shown in fig. 4.2 above

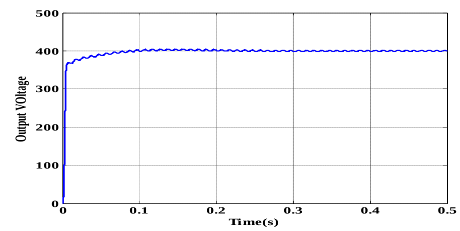

Fig. 4.3 Output voltage waveforms of the boost rectifier switched by the PSM at **R=650Ω**

For 650 ohms of resistance , output voltage waveforms are as shown in fig 4.3 above

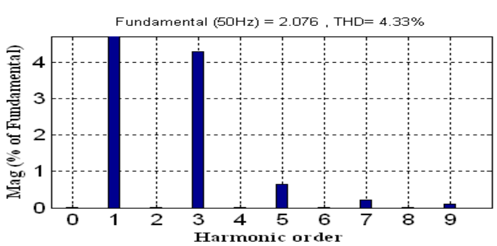

Fig. 4.4 Harmonic spectrum of the source current at R=650Ω

For 650 ohms of resistance , Harmonic spectrum is as shown in fig 4.4 above. and THD is 4.33%

For 350 Ohm

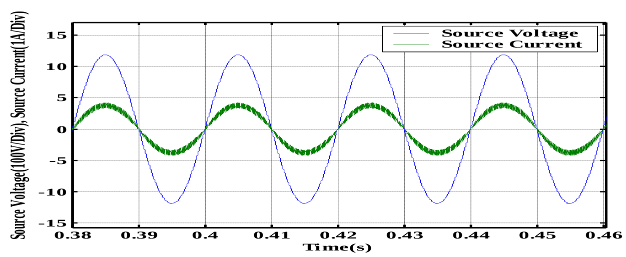

Fig. 4.5 Source current and voltage waveforms of the Boost Rectifier switched by the PSM at R=350Ω

For 350 ohms of resistance , source voltage and source currents are as shown in fig. 4.5 above

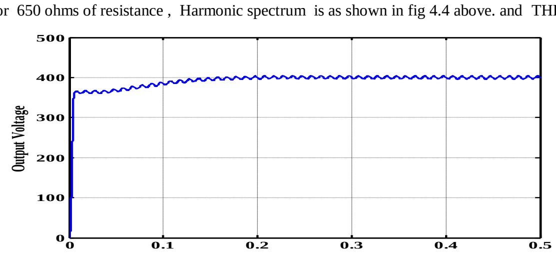

Fig. 4.6 Output voltage waveforms of the boost rectifier switched by the PSM at R=350Ω

For 350 ohms of resistance , output voltage waveforms are as shown in fig 4.6 above

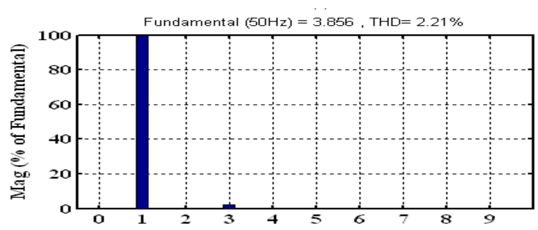

Fig. 4.7 Harmonic spectrum of the source current at R=350Ω

For 350 ohms of resistance , Harmonic spectrum is as shown in fig 4.7 above. and THD is 2.21%

REFERENCES

[1]. O.Garcia, LA. Cobos, R. Prieto, P. Alou, J. uceda, "Power Factor Correction: A Survey", IEEE Trans. Power electron., 2001,pp.8-13.

[2]. Ned. Mohan, Tore M.Undeland, Williams P. Robbins, "Power Electronics Converters, Applications and Design", John Wiley & Sons (Asia) Pte Ltd. Second Edition, 1995

ISSN (Print) : 2320 – 3765
ISSN (Online): 2278 – 8875

International Journal of Advanced Research in Electrical, Electronics and Instrumentation Engineering
Vol. 2, Issue 7, July 2013

[3]. Zheren Lai, Keyue Ma Smedly, “A Family of Continuous Conduction-Mode power- Factor-Correction Controllers based on the general pulse-width modulator”, IEEE Trans. On power electronics, Vol.13, no.3, May 1998,pp.501-510
[4]. Robert Mammano “Switching Power Supply topology, Voltage Mode Vs Current Mode”, Unitrode Design note. DN-62
[5]. Lioyd Dixon “Average Current Mode Control of Switching Power Supplies” Unitrode Design note. DN-140
[6]. J.P.Gegner and C.Q.Lee,’ Linear peak current mode control: A simple active power factor correction control technique for continuous conduction mode”, in Proc. IEEE PESC’96 Conf., 1996, pp.196-202.
[7]. D.Maksimovic, Y.Jang, and R.Erikson, “Non-linear carrier control for high power factor boost rectifiers”, Proc. IEEE APEC’95 Conf., 1995, pp.635-641.
[8]. Souvik Chattopadhayay, V. Ramanarayanan, and V. Jayashankar, “A Predictive Switching Modulator for Current Mode Control of High Power Factor Boost rectifiers”, IEEE Trans. On Power Electronics, vol. 18, No.1, Jan. 2003
[9]. Unitrode Application Note “Modeling, Analysis and Compensation of the Current Programmed Converters”, U-97
[10]. R.D. Middlebook and S.M.C’ui, “A general unified approach to modeling switching converter power stages,” in Proc. IEEE PESC’76 conf., 1976, pp. 18-34.

BIOGRAPHY

DR. K.RAVICHANDRUDU obtained his Ph.D from S.V.University,Tirupathi in 2012 and his area of interest are in Powersystem engineering, electrical machines.

M.SAILAJA is a PG student of Chadalawada Ramanamma Engineering College, Tirupathi. Her Area of interest are in Power Electronics and Drives.

M.MEENA is a PG student of Chadalawada Ramanamma Engineering College, Tirupathi. Area of interest are in Power Electronics and Drives.

P. SUMAN PRAMOD KUMAR, obtained his Bachleor’s degree from NBKR IST, Nellore Dist IN 2003 & Master’s Degree in 2005 from Bharath Institute of Higher Education & Research, Chennai. Presently Working as Associate Professor of EEE in chadalawada Ramanamma Engineering College,Tirupathi, Andhrapradesh. His area of interest are in Control Systems, Electrical Transmission & Distribution System & High Voltage Engineering.